Understanding the antenna response to obtain absolutely calibrated lightning measurements with LOFAR

Bachelorarbeit aus der Physik

Vorgelegt von
Klaus Hübner
September 22, 2022

Friedrich-Alexander-Universität Erlangen-Nürnberg

Betreuerin: Prof. Dr. Anna Nelles

Contents

1 Introduction

Lightning is a phenomenon that has been existing on our planet for as long as human kind. They even can be found in our solar system and probably on planets outside of our solar system. With a plasma temperature hotter than the surface of the sun, lightnings are a terrifying and at the same time very beautiful event. They can be found on earth, with a peak of four per second [10]. Even if they are so common in our atmosphere, they still remain *"[...]one of the most energetic processes in our atmosphere[8]."*
Despite of their destructive force and their long existence humans always admired them, but were still frightened. Our kind always searched for an explanation for flashes. Some of our ancestor's explained them with higher creatures, that they named God and prayed to. Even with thousands of years living with them and observing them, lightnings they are not well understood by scientists. But with big progress in observing radio waves and therefore expanding the technical limits, the option of understanding them comes closer. So most of the progress was done in the last 30 to 40 years of research[13]. With that increasing rate of knowledge gain it probably will not take as much time as it took to get to that knowledge.

One of the experiments that will help and has helped to understand lightning, since its start of observation in 2010 is the Low Frequency Array LOFAR. With its stations all over Europa it is the biggest telescope of the world at that low frequencies. Due to LOFAR it is possible to get measurements of lightning with an unprecedented resolution for lightning measurements, for example it could show that flashes observed in the Netherlands are quite different from the ones observed in the USA. In fact the charged layers of a cloud and therefore the propagation of the lightning stroke are the opposite of each other[17].

Therefore this thesis aims for a better understanding of the antenna response currently used at the LOFAR and change the existing code of the antenna response to work with a more accurate model of the low band antennas used at the Core of LOFAR. This will be tried by measuring the impedance and gain of the low noise amplifier of the antenna and using these data to improve the antenna model. At first I will give a general overview of the LOFAR telescope. Then I will describe the antenna used to detect the low band of LOFAR. To give a general understanding how lightning is measured I will give a brief over the source finding. To get a better understanding of the amplifier used in the LBAs the measurements of the amplifier and therefore the measurement needed components will be discussed. Last but not least I will talk about the used antenna model and add the measured data to the existing code. In the end I will give a quick summary and talk about the future development of this work.

2 LOFAR & Lightning

That chapter is about the Low Frequency Array and the way it is build. A closer look is taken at the used antennas, as well how it performs measuring lightning.

2.1 LOFAR

Fig. 2.1: Central core station in the Netherlands of LOFAR. From [11].

LOFAR (Low Frequency Array) is the largest radio telescope at low frequencies, built by the ASTRON institute. The goals of LOFAR is to observe the Dark Age, before stars and galaxies existed, the Epoch of Reionization (EoR), when gases were completely ionised by stars, also Deep Extragalactic Surveys and transient sources and pulsars, as well Ultra-high energy cosmic rays and Solar science, space weather and Cosmic magnetism. As well it was known by building LOFAR that it would be able to detected lightning. It achieves this dimensions with over 52 stations all over Europe.

The main, 38 of them are placed over 3.200 km^2 in north of the Netherlands. The main core, or also called the Superterp, with 24 stations is near Exloo. These are positioned in a 300 m circular area. The other 14 (remote) stations are scattered in the north of the Netherlands. The rest is placed in 7 other countries in Europe. Six in Germany, three in Poland and one each in France, Ireland, Latvia, Sweden and the UK. It works by virtually connecting all their stations to one big telescope, not like older single dish telescope. The central core of processing placed in Groningen. LOFAR is using at all stations lots of small antennas. It is operation frequencies are at 10 MHz to 240 MHz. With this it is the telescope with the lowest possible operating range on earth due

to our atmosphere [11, 17].

There are three different classifications of stations Core, Remote and International, each type with different electronics and field configurations and locations. The Core has 24 stations with each 96 low band antennas (LBA) and 48 high band antennas (HBA), one LBA is shown in Figure 2.1. HBAs are split into two fields of antennas. Both fields can add their 24 HBAs to one digital together. While all HBAs are still able to work as individual antenna. Each remote station has only one HBAs field, that contains all 48 HBAs. One remote station contains also 96 LBAs. International stations contains also 96 LBAs and one field of HBAs with 96, double the amount then the other stations types. The main difference to the other countries stations, is that the Dutch stations only have half of the digital receiver units for their LBAs. Therefore they Dutch ones only can use 48 dual polarization dipoles and the international ones the full capacity of 96 dual polarization dipoles [12].

Project AARTFAAC (Amsterdam-ASTRON Radio Transients Facility And Analysis Center) is a project fore making a picture of the visible sky every second. Therefore it uses 576 individual antennas. It is designed to observe black holes and neutron stars. The resolution of the generated pictures is 10 arcseconds, which does not correspond to its real capability. The maximal resolution of the LOFAR therefor is only usable for a small part of the sky at once [1].

2.2 Antenna

For observing the sky LOFAR uses LBAs Low Band Antennas and HBAs High Band Antennas and can observe frequencies from 10 MHz to 100 MHz, but are designed to work optimally in 20 MHz to 80 MHz. Fort the high band antennas the optimal range is 120 MHz to 240 MHz. Because the interference with the

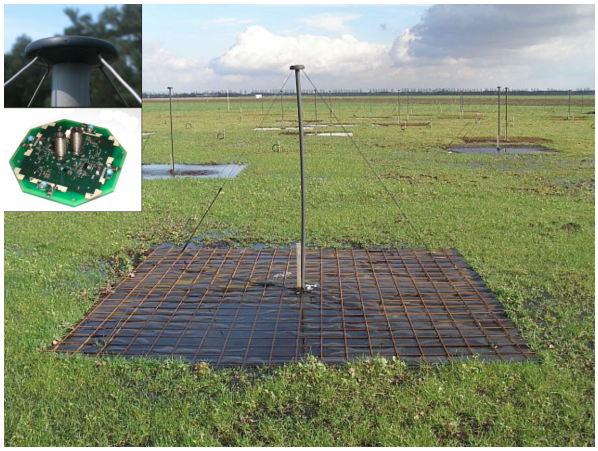

Fig. 2.2: Low band antenna picture with the amplifier on top of the pole, shown in the little picture top left and the electronics of the LNA underneath. From [5].

ionospheric reflection, RFI, is too large under 20 MHz so that the operating range need to be cut on the lower end to 20 MHz. At 90 MHz the FM band starts, so the observing frequency range was limited to 80 MHz [2, 14].

As shown in Figure 2.2, the antenna has four copper wires that are connected with an low noise amplifier (LNA) and they constitute the sensitive part of the antenna. A rubber band that is connected with the end of the wire functions as a spring and holds it on tension to have as less vibration in the wires as possible. They hold the wires are hold in an angel of 45° to ground and to the pvc pipe holding the amplifier. Through the coax cable the Low Noise Amplifier (LNA) gets its power past and through the same cable is the signal send, a bit more on that in section 3.2. To prevent damage by vegetation the LBAs are shielded with a foil, that is laid beneath them. More technical details are in section 4.1 [15, 2].

After its constantly recording data its not only picking up the electromagnetic waves from extraterrestrial sources, it also picks up every thing in the visible sky. In case of a lightning it so fore picks up the emitted frequencies of it.

2.3 Measuring Lightning

These emitted signal of lightning is formed in plasma channels which propagate in positive and negative, so called, leaders. The negative ones emit electromagnetic pulses in the $30 - 300$ MHz frequency band. Which correspond to the observable range of the LOFAR. The positive leaders only emits very little in the higher frequencies and could never been measured [7].

With the LOFAR a horizontal accuracy of 2 m are possible. With locating one event per microsecond [7].

To detect the sources with this high accuracy over distances, up to 100 km the calibration needs to be at nanoseconds level. Therefore the reference antenna in the core of a LOFAR station is used. The incoming data of each antenna are put in five nanosecond long blocks, which all overlap. Out of the blocks of data we find the four strongest pulses. The source position is found with a *"[...]minimize of the root mean square time difference (RMS) between the calculated arrival times and measured arrival times for all antennas[...]"* [17]. The chosen ones are compared with the measured ones in the close by antennas, which are arranged in rings in the Netherlands. If there are any equivocalness between the potential calibration pulse and other ones, that pulse is not used for calibration. In iterations all antennas are searched and the pulse source is searched for and based on the searched antennas updated. If a antenna is significantly different to the overall timing guess it will not been used. To calibrate each station the location of the source and the antenna timings are fitted together. This is performed for each station [17].

To find the final location of the source the flash is divided into 5 ns blocks. For each block the strongest pulses of reference antenna is searched for and sorted. If they have dual polarization and have a difference of 100 ns. By minimizing, like mentioned before, over the antennas of the Superterp the point of the source is located. Is one source found the next pulse will be calculated [17].

After performing this for the whole flash a figure, as shown in Figure 2.3, can be produced.
As mentioned at that point only Low Band Antenna (LBA) are used for the lightning research, which is why in the following only the LNAs of the LBAs are discussed.

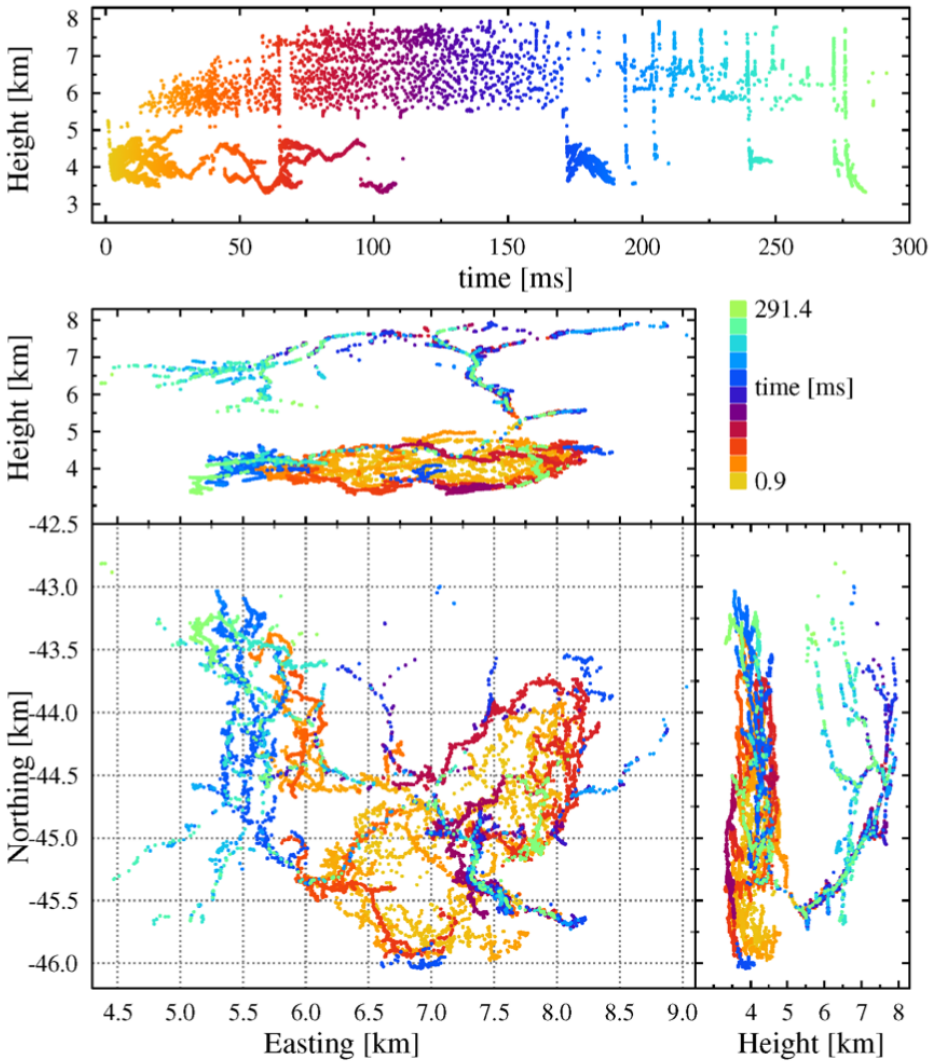

Fig. 2.3: Image of a lightning measurement from the year 2018. The larger upper panel is the height of the measured source against time. The color scale indicates the time. The central one is distance in the north over east direction with the LOFAR core as point zero. The smaller upper panel and the right one shows the height for each direction. From [17].

3 Amplifier measurement

Until now the amplifier of the LBAs are only taken into account by approximations of the impedance and the capacity of LNA in the code which models the antenna response. But the LNAs have a big influence on the outcome of the signal. So to improve the capabilities of the model a measurement of these two parameters is performed. Therefore this chapter will look at the measurement of the low noise amplifier and discuss the results. Since two additional components a bias tee and balun are necessary for the measurement of the amplifier the will be discussed too.

3.1 Measurement Setup for the LNA

To describe the LNA its impedance, the AC resistance, and gain need to be measured. Therefore the LNA was measured with an vector network analyzer (VNA). The VNA analyses a system which is connected by measuring the reflation of the signal puts it in respect to the not scattered signal over a given frequency range. These ratios are called scattering-Parameters (S-Parameters). [19] Out of these S-Parameters the impedances (Z-Parameters) can be calculated:

$$Z = \sqrt{z}(1_N + S)(1_N - S)^{(-1)}\sqrt{z} \tag{3.1}$$

with S the S-Parameters and z the characteristic impedance at each port of the VNA, in this case $z = 50\,\Omega$.

The measurements took place on three days, the ones of the first day will be ignored because the results were found to be incorrect.

A few preparations were necessary to perform the measurements. In perpetration for the second day the cables were soldered with a 1:1 balun which split the send signal into two for each antenna wire one to the antenna wires of LNA an connected with port one. The output power of the VNA was set to $-30\,\mathrm{dbm}$ as a standard output. In total were sixth measurement performed on the second day. The first one was performed with no voltage, but will not be discussed, after that the voltage was set to $8\,\mathrm{V}$ for the other measurements. For the third and fourth measurements the output power was varied. Fore the third it was lowered to $-60\,\mathrm{dbm}$ and for the fourth raised to $-10\,\mathrm{dbm}$. For the last two the output power was reset to $-30\,\mathrm{dbm}$ and the temperature around the LNA was lowered to $-20\,^\circ\mathrm{C}$ and then heated to $40\,^\circ\mathrm{C}$.

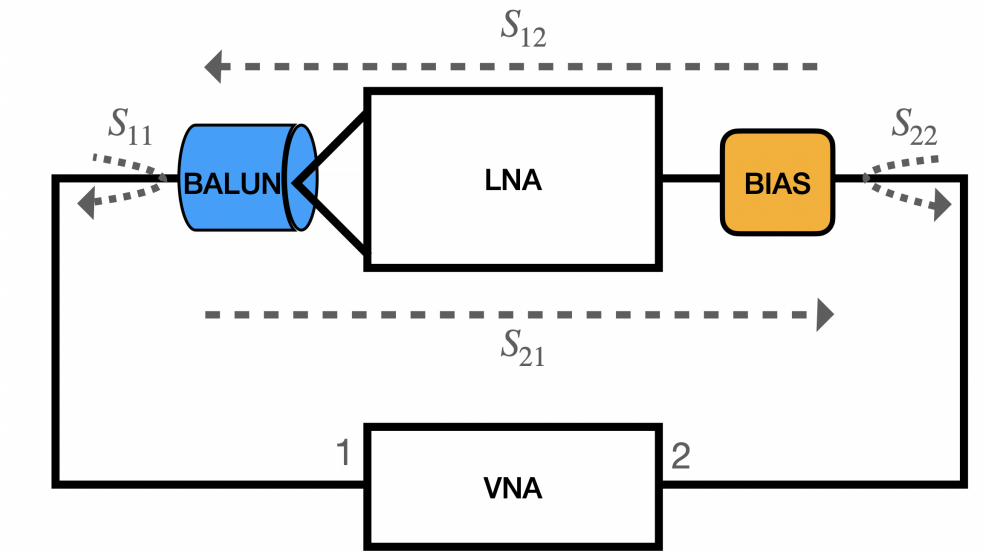

Fig. 3.1: Sketch of the measurement setup for the LNA of the antenna with the paths of the measurement sketched in and numbered. The ports of the VNA are numbered, too.

On day three the measurements where carried out with another balun and a $75-50\,\Omega$ bias tee. The measurement setup had a 1:1 balun on the first port of the VNA and then two of the antenna wires from the LNA were connected with the balun. After the LNA a $75-50\,\Omega$ bias tee was connected and the output of the bias is connected to the the second port of the VNA. A sketch of the setup was shown in Figure 3.1. The bias tee and the balun were measured with additional measurements to be able to see their influence on the total result. The results of the bias tee are discussed in section 3.2, the ones of the balun in section 3.3. The measurements of the LNA are discussed in section 3.4.

All the data were measured in a unit less Voltage Ratio to make the use in the code later easier.

3.2 Bias Tee

In order to deliver DC power to the amplifier of the antenna without interference with the signal a $75-50\,\Omega$ bias tee is needed which matches the cable and the LNA impedance. A bias tee delivers DC power on the port where the radio frequency signal is put in. So the characteristics of the used one on day three needs to be measured. [4]

3.2.1 Measurement Setup Bias Tee

To measure the bias tee the wires were connected as numbered in the sketch Figure 3.2, the power path is shown in the sketch as well. For the measurements the DC port of the bias was connected with the third port of then VNA. For the measurements of the $75-50\,\Omega$ bias tee the $75\,\Omega$ were connected at the

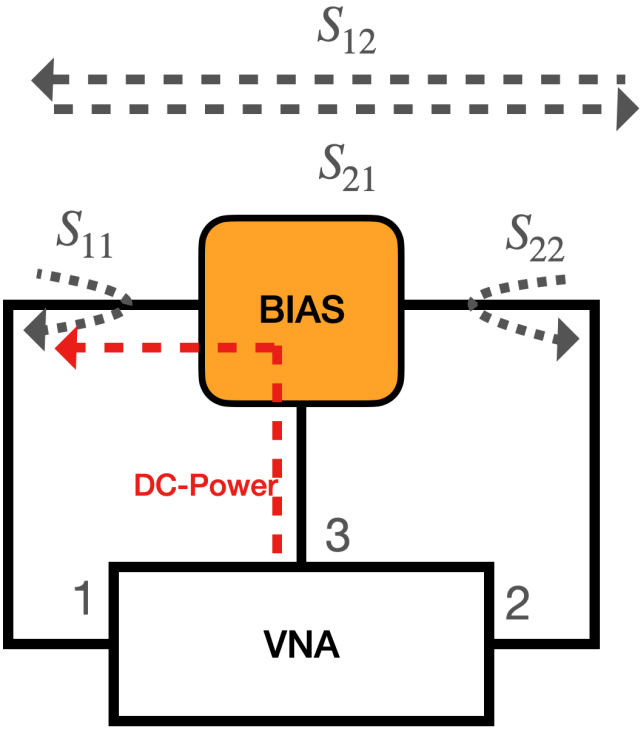

Fig. 3.2: Sketch of a BIAS with numbered in- and outputs of the VNA. As well Signal and DC-power path sketched in and numbered.

first Port, which functions as the IN port and a 50 Ω at port two, which was the OUT port, the bias IN was open. Two measurements were performed with it. One with only the first and second port connected and the other was done as a three port measurement. Port three was used as input. Therefore these both the measurements have for all the plot nearly the same shape and order of magnitude.

3.2.2 Measurement of the Bias

In order to know how the signal scatters at the input port the input match return (S_{11}) of the bias, shown in Figure 3.4, needs to be looked at. It appears flat and straight as well relatively small over the whole frequency range and therefore good. Next the reverse path of the signal needs to be looked at to see how much of the signal comes back to the input. The so called reverse isolation, represented by S_{12}, illustrated in Figure 3.4, is constant over the whole frequency range and around 0.48. Most interesting for the signal path is the way from the input to the output, S_{21}. The measured signal in this path is the gain of the path. In the case of a bias tee that lets the signal pass through is the same as S_{12}. Looking closer at the gain of the bias tee in Figure 3.5, it wiggles a lot, but is also nearly a straight line, which is the expected trend. To have less loss in signal strength the gain could be higher to have less effect on the gain of the whole measurement setup.

The last scattering parameter that needs to be looked at is the scattering at the output. The output match of the bias (S_{22}) is shown in Figure 3.5. That one is very low and slowly raises over the frequency range, but only ab bit.

As described before the impedance of the bias tee was calculated and must be looked at too. There are only two ones out of the four that are interesting for us. The first is the impedance of the input port, shown in Figure 3.6, which so is the resistance that the signal sees by entering the bias. The impedance starts fore the low frequency of 10 MHz at around 113 Ω and falls to nearly 50 Ω at the upper end of the LBA frequency range. The second impedance of interest is the one between the two ports (Figure 3.6), which falls as well down to nearly 50 Ω at the end, but at the lower end of the frequencies at a lower value around 73 Ω and has a more curved shape in the beginning and the end. Therefore the impedance change over the whole frequency range, but is in the end not so dominant that it will influence the measurement.
In order to know what is the delay time of the signal for the frequencies coming trough the bias tee this is plotted as well and is shown in Figure 3.7. It wiggles a lot over the whole frequency range, but no frequency needs particular more time to pass through.

The last thing to look at of the bias tee is the isolation of the DC-Path, illustrated in Figure 3.3, it is apparent that it is very good. It starts low for 10 MHz and only raises oft until 90 MHz, for the four possible paths S_{31}, S_{13}, S_{32} and S_{23}. The reverse way of S_{31} and the one for S_{32} are both very similar like expected. Therefore no strong influence of the bias tee should be expected. It can be concluded that the bias tee is not really influencing the measurement of the LNA.

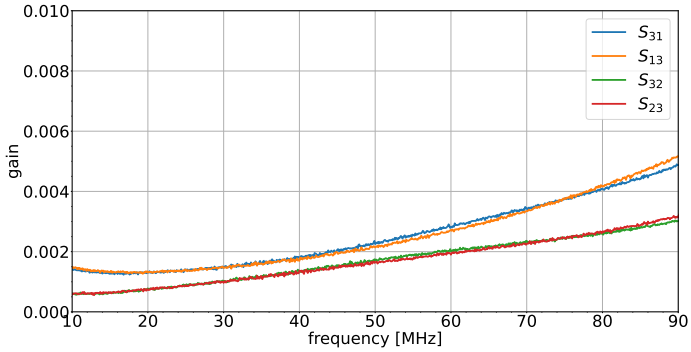

Fig. 3.3: Isolation of the DC-path S_{31}, S_{13}, S_{32} and S_{23} of the bias.

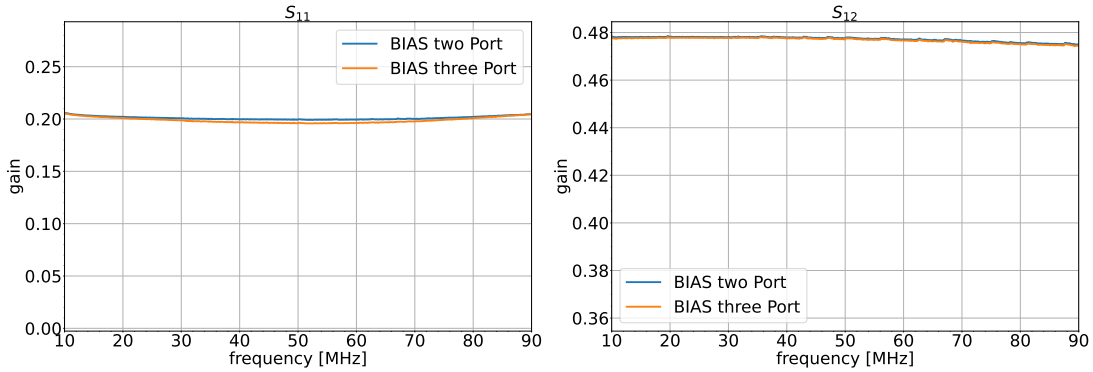

Fig. 3.4: Left the input match return S_{11} and on the right the reverse isolation S_{12} in gain of the S-Parameter versus the frequency of the bias measured on the third day.

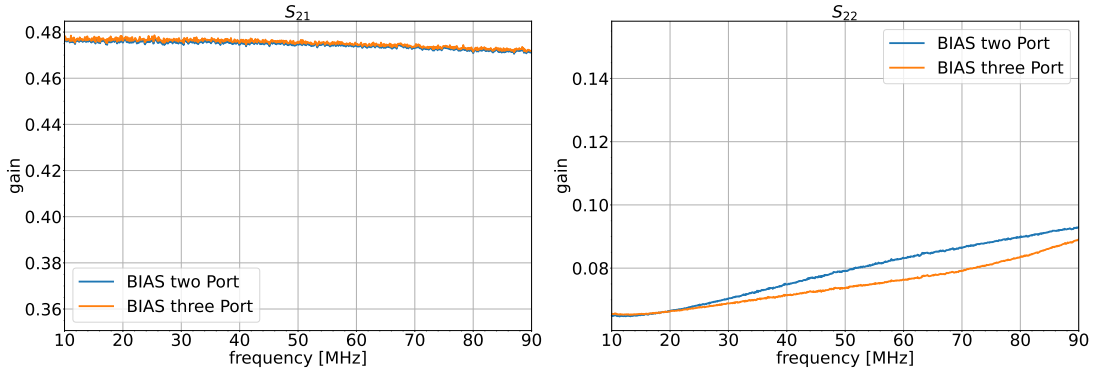

Fig. 3.5: Left the gain S_{21} and right the output match S_{22} in gain of the S-Parameter versus the frequency of the bias measured on the third day.

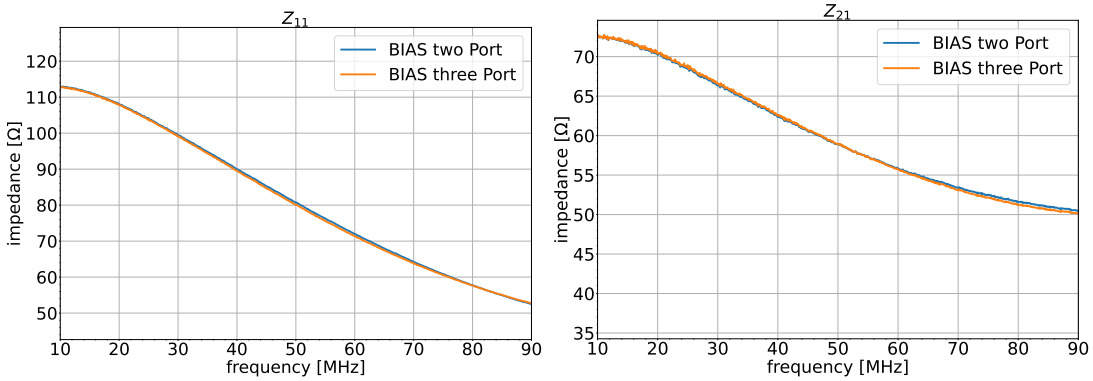

Fig. 3.6: Impedance of the input Z_{11} on the left and on the right the impedance Z_{21} between the ports versus the frequency of the bias.

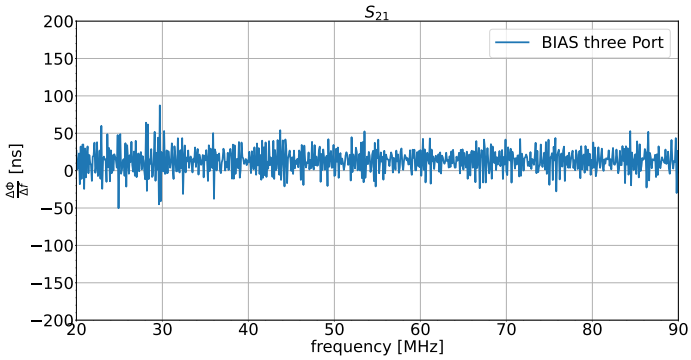

Fig. 3.7: The group delay of the path of the signal S_{21} of the bias in nanoseconds versus frequency.

3.3 Balun

The balun is *"a device that converts between balanced and unbalanced electrical signals, esp. from an unbalanced coaxial cable to a balanced antenna."*[3] Since the balun is a component of the measurement and therefore can influence the measurement significantly the balun of the third day was measured separately, too.

3.3.1 Measurement Setup Balun

The two measurements were carried out with different bendings of the cable to see how the measurement depends on the coupling between the wires. As port one the sma in was used. The positive side of the balun was port two.

3.3.2 Measurement of the Balun

As before the input match and output match had to be analysed at in order to see how much of the signal scatters on the ports. They are shown in Figure 3.8. They appear quite different according to the bending and therefore they could be better. Also the reflection on the input port is relatively high.

The most relevant S-parameter the gain (S_{21}) and reverse isolation (S_{12}) of the balun are high, like at the bias tee, the balun only lets signals through, so there is not a big difference between the two curves expected. Both are shown in Figure 3.9. Both starting by around 0.68 going down in a slight curve to around 0.64 and S_{12} appears noisier than the gain, but both change only a little bit over the frequency range, which is not ideal for a good measurement. The gain should be higher for a good measurement, so that there are less losses in the signal chain. But S_{12} and S_{21} only show a little dependence on the bending of the cable.

The same appears in the important impedances Z_{11} and Z_{21}, illustrated in Figure 3.10. They show a pretty high dependence on the frequency. With Z_{11} starting high slightly above 500 Ω for the lower frequencies and then falling

down to around 150 Ω for the higher end. For Z_{21} the curve starts at around 250 Ω and falls down to around 140 Ω. But they don't change that much with the bending. Therefore the overall frequency dependence of the balun and the high impedance is way to big too not influence the measurement in a dominant way.

At last it is necessary to analyse the time the signal needs to go through the balun. The group delay of the balun, shown in Figure 3.11, does not change with the bending, and appears noisy, but the overall trend is constant, so like with the bias tee no frequency area needs significantly more time to reach the other port.

Therefore the balun is not ideal to perform optimal measurements of the LNA.

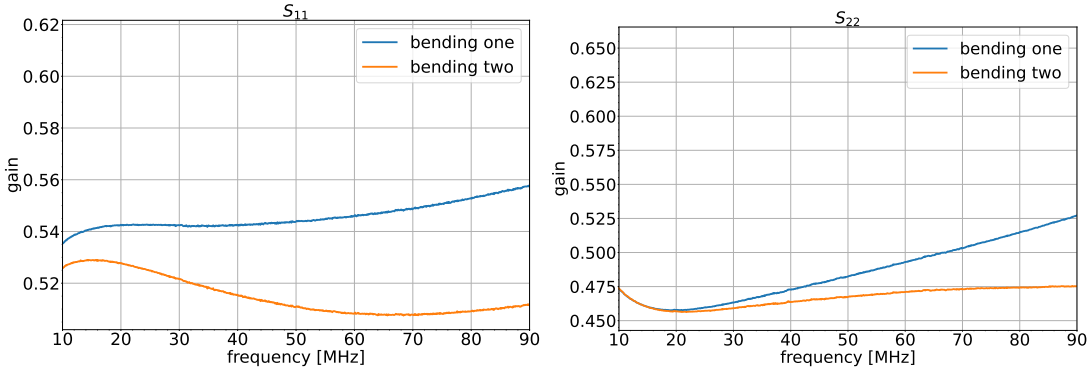

Fig. 3.8: Left the input match S_{11} and on the right the output match S_{22} in gain of the S-Parameter versus the frequency of the balun measured on the third day.

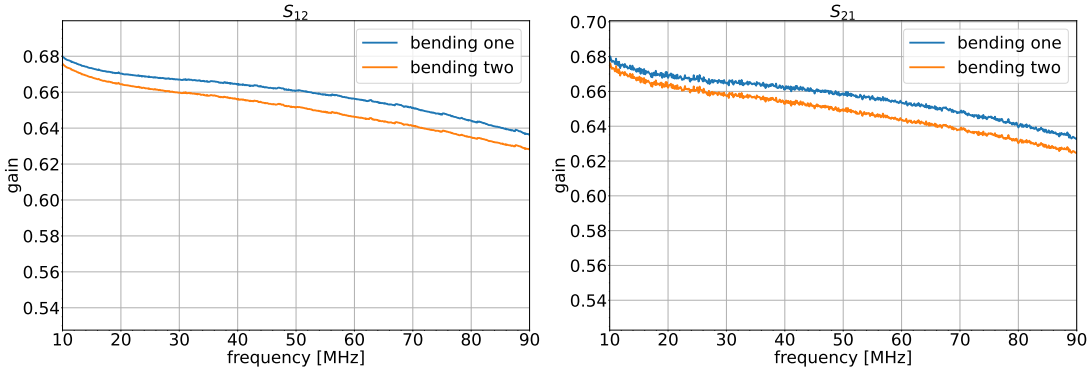

Fig. 3.9: Left the return loss S_{12} and on the right the gain S_{21} in gain of the S-Parameter versus the frequency of the balun measured on the third day.

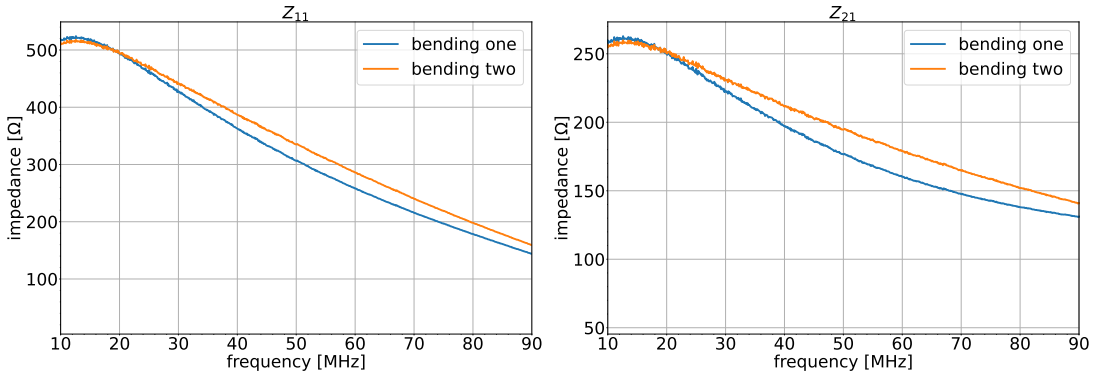

Fig. 3.10: Impedance of the input Z_{11} on the left and the right the impedance Z_{21} versus the frequency of the balun.

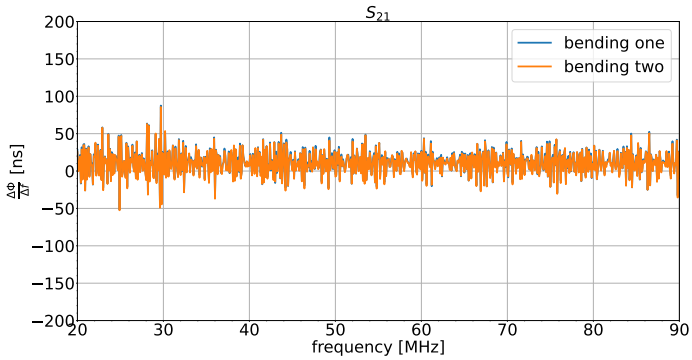

Fig. 3.11: The group delay of the path of the signal S_{21} of the bias in nanoseconds versus frequency.

3.4 Measurements of the LNA

Here are the data obtained for the hole setup, previously described in section 3.1 and shown in Figure 3.1.

Starting again with the input match return loss (S_{11}). It shows that the reflection at the antenna wire input for all measurements follows nearly the same curve, as shown in Figure 3.12. For end of lower frequencies the amplitude is lower at around 0.4 and goes then up to nearly 0.9 at the upper end of the frequency range of the antenna and shows after that a visible drop. So for lower frequencies the scattering is better than on the upper end.

Compared with the measurement done on day three, shown in Figure 3.12, the curve is completely different to the the curves of day two. The measurement is a straight flat line, at around 0.85 for the most of the frequency range from 10 MHz up to around 80 MHz, but then it has also a drop which is much harsher then the one of the measurements done on day two. The drops are both related to the inner structure of the LNA, because of the measurement range of the LBAs, which is cut at 80 MHz it does not influence the antenna response and

is therefore no problem. But the overall height of the back scattered signal is lager than expected, but could come from the fact that the LNA is output matched.

The reverse isolation (S_{12}) should be in an ideal case 0, but as shown in Figure 3.13, the isolation obtained on day two is not perfect. There is a quite small signal coming back, so it is a good enough isolation for the way back. Only for a low power output of -60 dbm the reverse isolation starts to get a little worse. On the other hand the measurement done on day three (Figure 3.13) shows a much much lower amplitude with a maximum of around 0.0005. Therefore the reverse isolation gives good results and only gets slightly worse for higher frequencies.

Now we consider the measurements taken during day two of the gain or loss for sending the signal from the antenna wire to the output of the amplifier(Figure 3.14). All measurements have the same gain amplitude, except the measurement with -10 dbm power output which has a visible lower amplitude. The other ones are all starting at around 4.0 for the lower frequencies and raise a little to continue with a flat line only to fall down at around 70 MHz and gets steeper at the higher end of the frequency range, due to the cut for higher frequencies. The gain seems not to be affected for the power output from -60 dbm to -30 dbm. Only the gain measured at $-20\,^{\circ}$C is a slightly higher then the rest, which lead to the conclusion that the overall gain in very cold days could have an effect, but should be miner.

Similar as before the course of the graph is much different, comparing day three and day two, like shown in Figure 3.14. The day three measurement starts a bit lower than the -10 dbm power output measurements of day two. Then the gain grows in a slight curve and reaches the highest point at around 85 MHz and drop quickly afterwards, but remains below the measurement overall gain of day two. As mentioned before the drops at higher frequencies and is not a problem or influence later on, due to the cut at 80 MHz. As expected the overall gain is higher then one, because the LNA amplifies the signal strength.

The remaining S-parameter S_{22}, the scattered signal at the output, is shown in Figure 3.15. On day two the amplitude for all measurements is small and is around 0.1 at the maximum. It starts for the lower end at around 0.05 and raises until frequencies around 50 MHz where it stays nearly level short under 0.1. Just the measurement -60 dbm appears noise again, but is at the same values as the others. The measurements obtained on day there remains under 0.025 with it lowest point at around 60 MHz. Its highest points is at the lower and upper end of the LBA frequency range. After it is out put matched it is expected to be that low.

The impedance of Z_{11} (Figure 3.16) and Z_{21} (Figure 3.17) is also interesting for the behavior of the antenna.

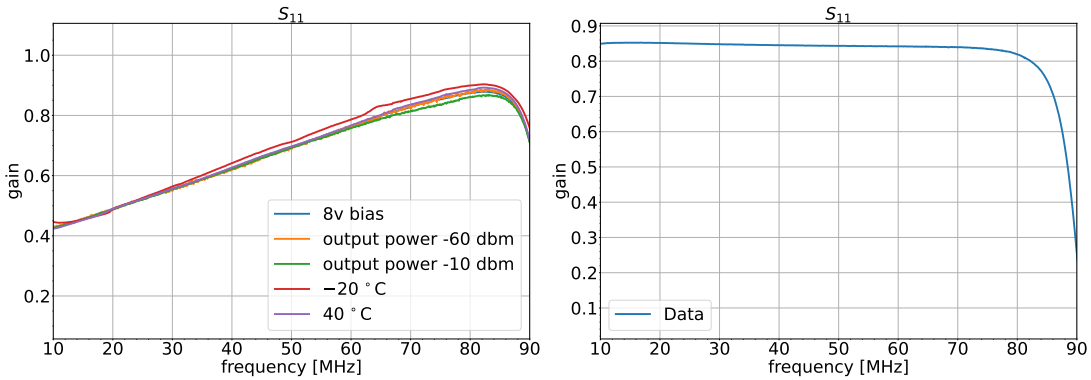

Fig. 3.12: The input match S_{11} in gain of the S-Parameter versus the frequency with left the second day and on the right third day of measurements.

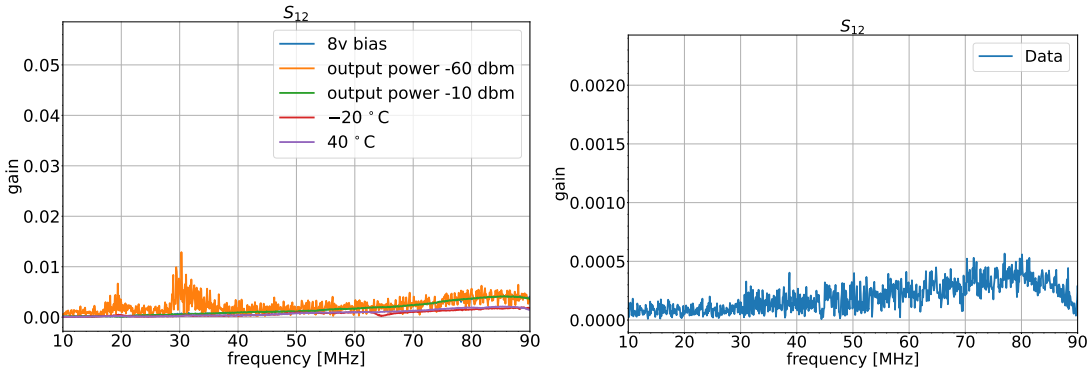

Fig. 3.13: The return loss S_{12} in gain of the S-Parameter versus the frequency with left the second day and on the right third day of measurements.

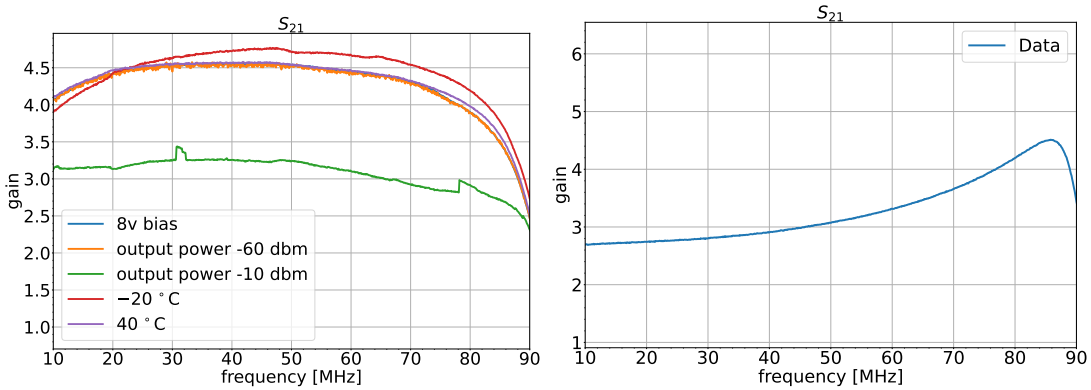

Fig. 3.14: The gain S_{21} in gain of the S-Parameter versus the frequency with left the second day and on the right third day of measurements.

The Z-Parameters were calculated from the S-Parameters with Equation 3.1. The impedance on the input Z_{11} of day two (Figure 3.16) shows a decreasing trend of the impedance for the frequency range of interest at 20 MHz to 80 MHz. The measurement data does not have the expected linear behavior. The measurement on day two it grows from around 110 Ω at 10 MHz to the maximum at nearly 20 MHz at around 140 Ω and reaches a local minimum close to 90 MHz. All measurements appear relatively close to each other only the lowest power out put at −60 dbm causes an impedance with an irregular trend. Only the measurement at −20 °C shows a drastic change in the impedance. It is lower for the lower frequencies and after crossing the highest point of the other measurements it has the maximum at bit after 20 MHz. The impedance stays higher then the others and reaches its minimum short before 90 MHz. Like in previous measurements only cold effects the measurements significantly.

Day three measurement, illustrated in Figure 3.16, looks like the measurements of the second day with no raise on the lower frequencies. The rest of the frequencies looks similar, just a bit stretched to the left. The highest point is at 10 MHz close to 600 Ω which is much higher impedance then measured on day two and reaches its minimum at 90 MHz with approximately 20 Ω. So the impedance is strongly effected by the frequencies.

The height of the Z_{11} of the balun, discussed in subsection 3.3.2 and shown in Figure 3.10 is of the same magnitude of the Z_{11} of the whole measurement setup which leads to the conclusion that the input impedance is strong influenced by the balun. After day two and day three uses different Baluns for the measurement a strong dependents on the balun is obvious because of the high difference in impedance values.

The impedance Z_{21}, shown in Figure 3.17, is the impedance between the two ports, where the signal passes through. Z_{21} and Z_{11} have a similar curve, but Z_{21} is higher. It starts at approximately 650 Ω and has a maximum at around 20 MHz like Z_{11} with nearly 850 Ω to decreases like the right side of a Gaussian to the minimum of 150 Ω at 90 MHz. Again the lowest power output has a noticeable influence on the curve. Like for the S-Parameter S_{21} the higher output power of −10 dbm has the biggest influence on day two. It lies much lower then the others measurements, starting at 500 Ω and staying below the other measurements of day two until the lowest point at 90 MHz. As in Z_{11} is the −20 °C measurement higher for the relevant frequency range from 20 MHz to 80 MHz. Looking at the plot from day three, illustrated in Figure 3.17 on the right, the course of the measurements is similar to the Z_{11} measurements of day two. However in this case the maximum is at 1700 Ω at 10 MHz and the minimum is at 90 MHz with 250 Ω.

The last thing to analyse is the group delay which represents the delay the signal obtains by passing through the measured components, illustrated in the group delay in Figure 3.18. On both days the curve appears noisy. On day two only the measurement with higher delays is the low power one with

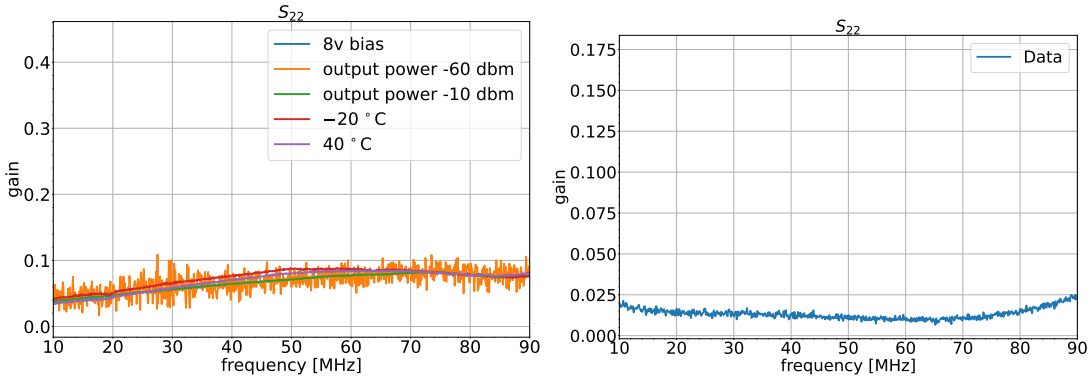

Fig. 3.15: The output match S_{22} in gain of the S-Parameter versus the frequency with left the second day and on the right third day of measurements.

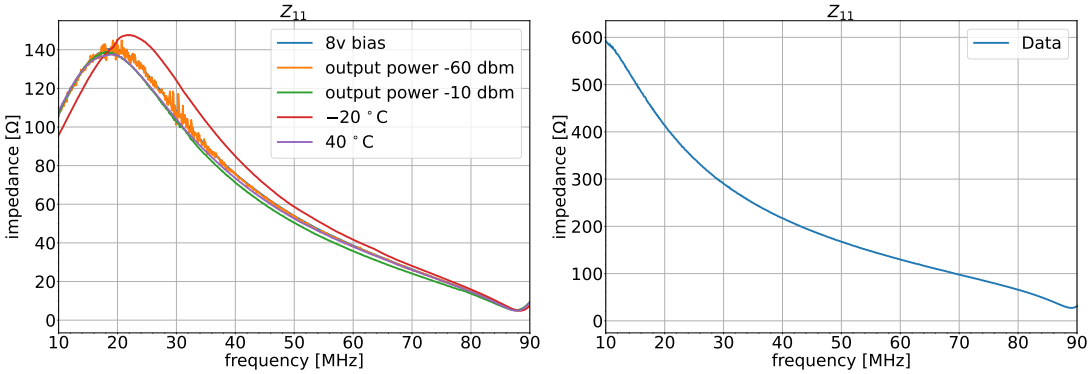

Fig. 3.16: Impedance of the input Z_{11} on the left day two and the right day three versus the frequency.

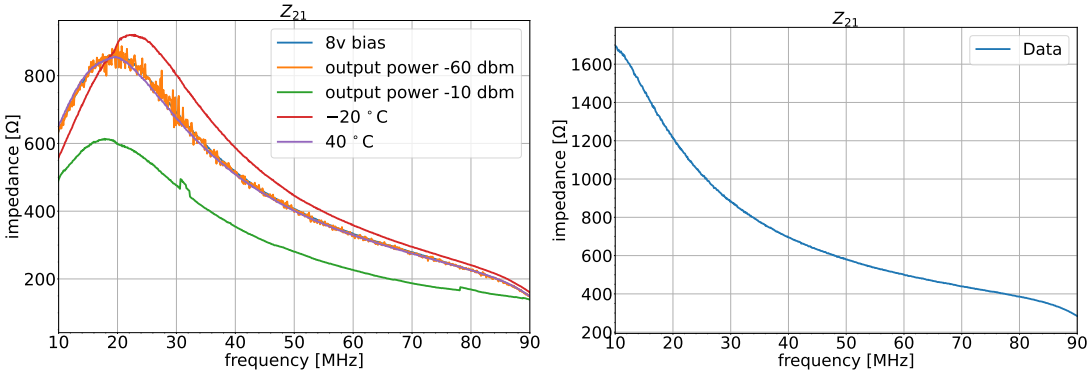

Fig. 3.17: Impedance of the input Z_{21} on the left day two and the right day three versus the frequency.

−60 dbm, the other measurements are similar. The plot shows that the higher frequencies after 85 MHz pass through the LNA quicker than the lower ones. That's much different to the day three measurement. This one has only a slight delay on the lower frequencies until 75 MHz after which the delay raises a bit to get much faster higher after 80 MHz, only at the end its again a lower. In the measurement of day three the lower frequencies arrive earlier than the high ones which need more then 10 times the time of the lower ones. But this will have no influence on the data due to the cut at 80 MHz.

In conclusion of the both data sets the two days obtained very different results. These differences are expected after the measurements on day three were done with a different balun. Also very low temperatures can have a small effect on the results, for the Core of LOFAR. But overall the measurement of the LNA is very much influenced by the used balun and therefore the way chosen and described for measuring the LNA with a balun as connector, which so turns out to be problematic.

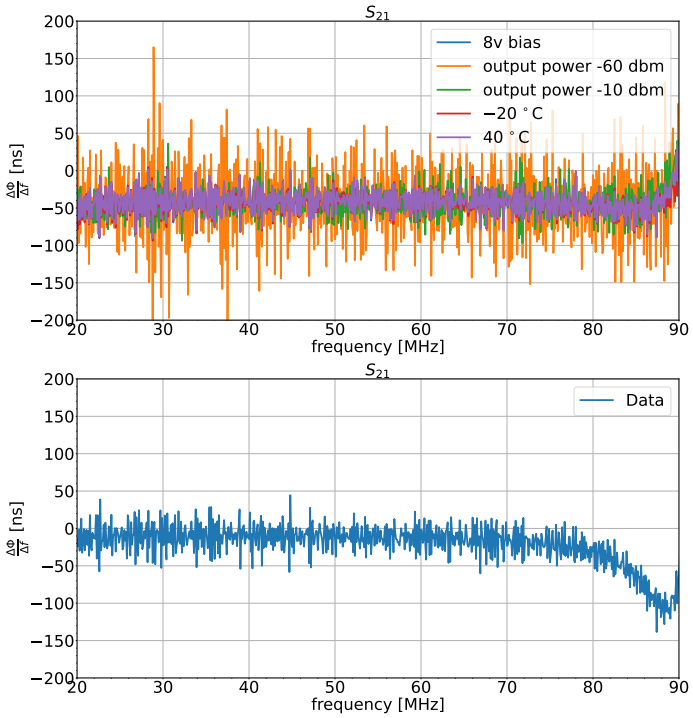

Fig. 3.18: The group delay of the path of the signal S_{21} in nanoseconds versus frequency, the delay of day two on the left and right day three.

4 Antenna Modelling

In this chapter is described the implementations of the measurements which is discussed in the previous chapter 3 in the antenna model code which can be found under [9]. To understand the code in a better way a closer look is taken at the technical details of the LBAs. Then the calibrations method, the preparation of the data and interpolation will be described. At the end the antenna response gets analysed and the calibration will be looked at. With the main goal to achieve a better calibration.

4.1 Technical details of the LBAs

In order to be able to improve the antenna response it is necessary to take a closer look at the technical details of the antenna and how it can be described.

To be able to pin point the location of one event in the sky it is necessary to have a coordinate system to work with. A visualisation of it is illustrated in Figure 4.1. The measured signal is dependent on two angles, called Φ and θ, which describe the azimuth and the zenith coordinates respectively. Which are given by two wires positioned so that they faces from southwest to northeast and the other two are perpendicular positioned southeast to northwest, as illustrated in Figure 4.1 indicated by X and Y. The incoming electric field can be described with the vectors $\hat{e}_\Phi$ and $\hat{e}_\theta$. The direction of the source with the perpendicular vector $\hat{e}_n$ [15, 6].

The signal measured by each individual antenna, at the X- and Y-dipoles, is called $\vec{S}_a$, and can be calculated into an electric field $\vec{E}_a$. Therefore the Jones matrix $J_a(\nu, \theta, \Phi)$ is needed. The Jones matrix takes into account the frequencies ν, the angles θ and Φ and describes the response of the antenna. a is the index of the specific antenna. The following equation calculates the voltage based on ideal circumstances [16, 6].

$$\vec{E}_a = J_a(\nu, \theta, \Phi)^{-1} \vec{S}_a \tag{4.1}$$

However the LNA of the LBAs has a variation over time, which needs to be taken into account with a factor $F_a(t)$, for each dipole of the antenna and also a calibration factor $C(\nu)$ is necessary. With that the Equation 4.1 could be rewritten as [6, 16]:

$$F_a(t)C(\nu)\vec{S}_a J_a(\nu, \theta, \Phi)^{-1} = \vec{E}_a \tag{4.2}$$

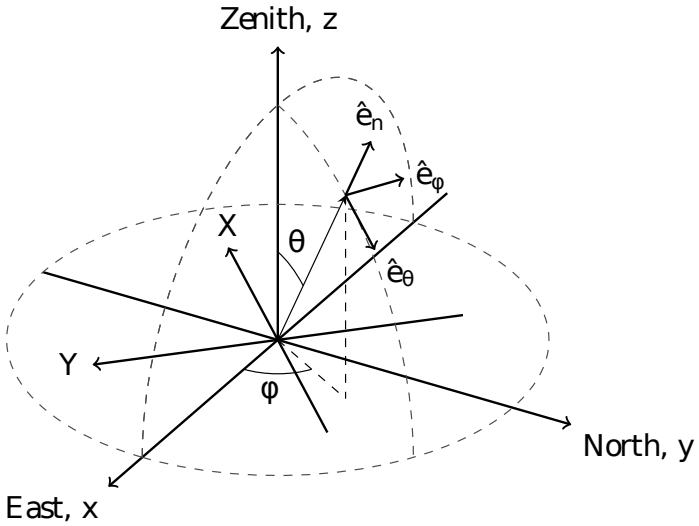

Fig. 4.1: Coordinate system to describe the low band antenna. Φ as the azimuth and θ as zenith angle. X and Y representing the alignment of the dipole wires. From [6].

The LBA amplifier can be simplified as illustrated in Figure 4.2. On the left side of the circuit represented with V_{emf}, there is the signal of interest and Z_a is the impedance of the antenna. The input impedance Z_{LNA} can be calculated with the resistor R and the capacitor C with $R = 700\,\Omega$ and $C = 15\,\mathrm{pF}$, which are the values that are found to produce the best antenna response. Z_{LNA} is given by [6]:

$$Z_{\mathrm{LNA}} = \frac{R}{1 + j\omega RC} \tag{4.3}$$

with $\omega = 2\pi\nu$ and ν the frequency. The gain of the system is marked with G_V. The output resistance of the LNA R_{out} and the output impedance Z_{out} needs to match the one of the used cables, which are commonly $75\,\Omega$ at LOFAR [15, 6].

The resonance frequency of the LBAs antenna cable, which are 1.38 m long, is 52 MHz, but the LNA shifts the resonance frequency to 58 MHz, to cover a bigger frequency range with lower noise [5].

4.2 Calibration

In order to calibrate the LBAs a known source is necessary. Therefore the galactic emission is used, because it is always in the background of the collected data. Also the electric noise of the LOFAR is taken into account to provide a good calibration. But the biggest influence on the calibration has the active antenna which is the first big influencing part in the signal path [14].

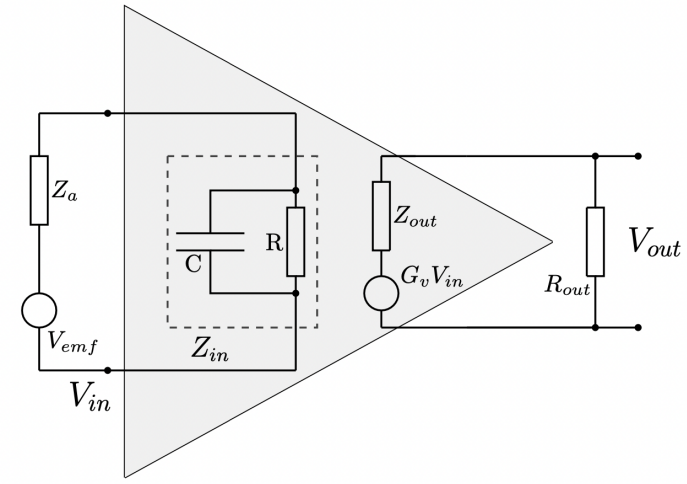

Fig. 4.2: Simplified circuit like the one which works in the LBA as LNA. With Z_{in} representing the input impedance given by C and R. Z_{out} is the output impedance and the Gain is marked as G_V. From [15].

4.3 Preparation

In preparation for the antenna model change the losses in the measurement setup must be taken in account, too. The balun and bias tee have gains that need to be considered in in the complete measurement, the gain of the whole set up is divided by the gain of the balun and the gain of the bias tee, shown in Figure 4.3. The so "cleared up" gain of the LNA is way higher than the one shown in Figure 3.14. This is expected, because the bias and the balun produces a loss in signal strength. Now it comes closer to the real gain of the LNA, which will be referred to as the gain of the LNA.

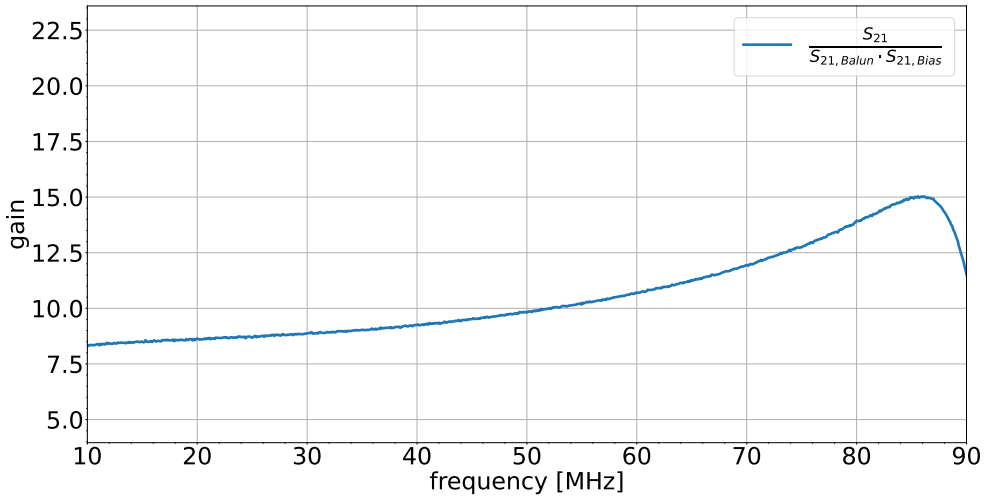

Fig. 4.3: The gain $\frac{S_{21}}{S_{21,Balun} \cdot S_{21,Bias}}$ in gain of the S-parameter versus the frequency.

4.4 Interpolation

The measurements, described in section 3.4, will be used to improve the antenna response. So before the changes are described, it is necessary to think about how data points with no information between these points are connectable. For this purpose, the python library scipy has a package called *interpolate* which includes different sub packages. This package is used to find a function best representing the data which are put in. For the purpose of a one dimensional function $y = f(x)$ the fit function is given by the class called *interp1d*. It is called as [18]:

```
scipy.interpolate.interp1d(x, y, kind='linear', axis=- 1, copy=True,
bounds_error=None, fill_value=nan, assume_sorted=False)
```

The *'linear'* and the *'cubic'* fit were tried to fit the data point. By plotting the both methods over the data no difference in the shape or the values is visible. Therefore the ratio of the two interpolations by dividing the *'cubic'* with the *'linear'* is shown in Figure 4.5. The plot shows that there is only a small difference between the two methods. The impedance plot shows a maximum difference of a 0.12 percent. The gain on the other hand shows a maximum difference of 0.14 percent between the two methods of interpolation. Since there is only a small difference for the impedance and the gain it is not really a difference, which method is chosen. So to be closer to the measured data the linear one will be used. The data points are also close enough to each other, with 10 data points per megahertz, to use the linear one for the impedance.

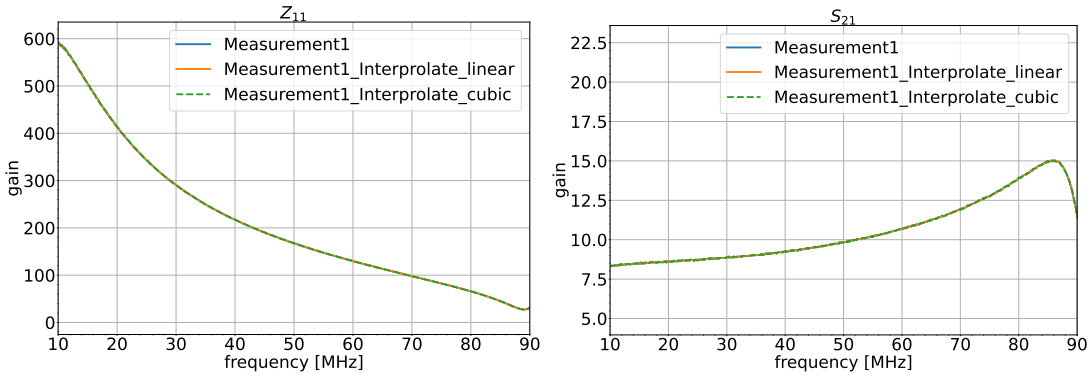

Fig. 4.4: Comparison of the two versions of interpolation for the new antenna response with the data points, plotted versus the frequency, by putting them on top of each other. The left one is the input impedance comparison and the right one the gain of the LNA.

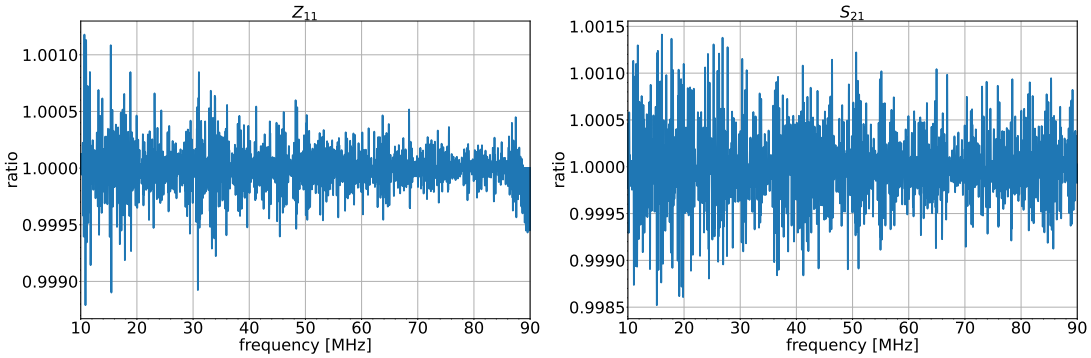

Fig. 4.5: Comparison of the two version of interpolation for the new antenna response plotted versus the frequency, by dividing the *'cubic'* interpolation with the *'linear'*. The left one is the input impedance comparison and the right one the gain of the LNA.

4.5 Antenna response

In this section the antenna response and the code itself will be discussed. To make it easier to work with the code and to change the code, Equation 4.2 can be rearranged into:

$$F_a(t)C(\nu)\vec{S}_a = J_a(\nu,\theta,\Phi)\vec{E}_a \tag{4.4}$$

This equation makes it easier as it is easier to see the base structure of the calculation in the code. The left side is now implemented to calculate a Jones matrix.

The voltage output $V_{out}(e_{field},\theta,\Phi,\nu)$ of the LNA can be calculated with Equation 4.5 with $Z_{\mathrm{LNA}}(\nu)$ the input impedance dependent on the frequency.. The voltage depends on electric field direction e_{field}, the azimuth angle θ and zenith angle Φ, as well as on the frequency ν. For better understanding of the real system a simplified Circuit is shown in the Figure 4.2.

$$V_{out}(e_{\mathrm{field}},\theta,\Phi,\nu) = Z_{\mathrm{LNA}}(\nu)\cdot(Z_{\mathrm{LNA}}(\nu)+Z_{\mathrm{ant}}(\nu))^{-1}\cdot G_z(e_{\mathrm{field}},\theta,\Phi,\nu) \tag{4.5}$$

Its form is a diagonal matrix. The values on the diagonal are calculated with the Equation 4.3 mentioned previously. The multiplied matrix $Z_{\mathrm{ant}}(\nu)$ is the mutual antenna impedance, which also depends on the frequency. The gain of the system is taken into account with the vector $G_z(e_{\mathrm{field}},\theta,\Phi,\nu)$. It depends on the electric field direction, the angle the signal is coming from and the frequency. Until now there were no good guess or information on what $G_z(e_{\mathrm{field}},\theta,\Phi,\nu)$ looks like, so it was not implemented [6].
The antenna response calculated with Equation 4.3 and Equation 4.5 will be referred to as old antenna response and the modified one will be called new antenna response. A plot of the Jones matrix over frequency of the old antenna response is shown in Figure 4.6. Since these R and C values used for

Z_{LNA} are only one value for the whole frequency range and they are found by taking the ones that describe the response best another solution is needed for a good calibration. Therefore the frequency dependent parameter Z_{LNA} and $G_z(e_{\mathrm{field}}, \theta, \Phi, \nu)$ of the Equation 4.5 needed to be measured, as performed and described in chapter 3.

To use the results in the existing antenna response code from the AARTFAAC LBA model it was necessary to add and change a section of the code. For the code to appear for other calls of the function unchanged the class call code was changed from,

```
def __init__(self, model_loc=None, R=700, C=15e-12, mode="LBA_OUTER"):
    if model_loc is None:
        model_loc = dirname(abspath(__file__)) + '/AARTFAAC_LBA_MODEL/'
```

, to

```
def __init__(self, model_loc=None, R=None, C=None, mode="LBA_OUTER"):
    if (R is None) and (C is None):
        r_c_Or_parameters = 'parameters'
        self.R = None
        self.C = None
    else:
        r_c_Or_parameters = 'r_c'
        if R == 'original':
            self.R = R
            C = 15e-12
            self.C = C
        else:
            if R != None:
                self.R = R
            else:
                R = 700
                self.R = R
            if C != None:
                self.C = C
            else:
                C = 15e-12
                self.C = C
            self.Z = None
```

where the code is able to be called like before. When no specific values for the resistance or the capacity are wanted it will run the new version with the measured parameters. In case the old version of antenna response is needed, the code will use the original version. Therefore the input parameter R needs to be given the string *'original'*. If only one of the resistance or the capacity should be changed individual then, the code will run the old version and make sure, that the not changed one have the best found value for the old antenna response as the old code did.

In the new antenna response the input impedance of the LNA $Z_{\mathrm{LNA}}(\nu)$ is replaced with the impedance measurement Z_{11} of the third day of measurements,

shown in Figure 3.16. The gain of the LNA system was also measured so that the $G_z(e_{\text{field}}, \theta, \Phi, \nu)$ can be replaced with the measurement of the gain of the signal passing through the LNA S_{21} of the third day of measurements, shown in Figure 3.14. The renamed function *set_LNA_behavior* which was called before *set_RC*, will load the data with the new version. In addition to the R and C value, which are now per default set to ***None***, which is also accepted by the function needs now a new parameter *r_c_Or_parameters*. This one is implemented to decide whether the new code will be used or the one depending on the R and C value.

The new version then loads the data which are stored now in the already existing directory *data* under a new folder for the measurements. The file stores the data in scattering parameters in unit less voltage ratios versus the measured frequencies. After sorting the S-parameters and saving the frequency separately, the S-parameter are converted into the impedances (Z-parameters), by using the Equation 3.1. Then the interpolation discussed in section 4.4 is implemented to connect the data points. After that the matrices are in complex values, but *scipy.interpolate.interp1d* only takes real values, it is necessary to convert the impedance before interpretation into Ohm. Therefore the absolute value of the values must be calculated. Then the impedance before calculated with Equation 4.3 is replaced with the new interpolated impedance data. If the new antenna response is calculated, also the gain $G_z(e_{\text{field}}, \theta, \Phi, \nu)$ which is the gain of the LNA of S_{21} and was not taken in account until now, is added to the function as mentioned in Equation 4.5.

4.6 Improvements & Results

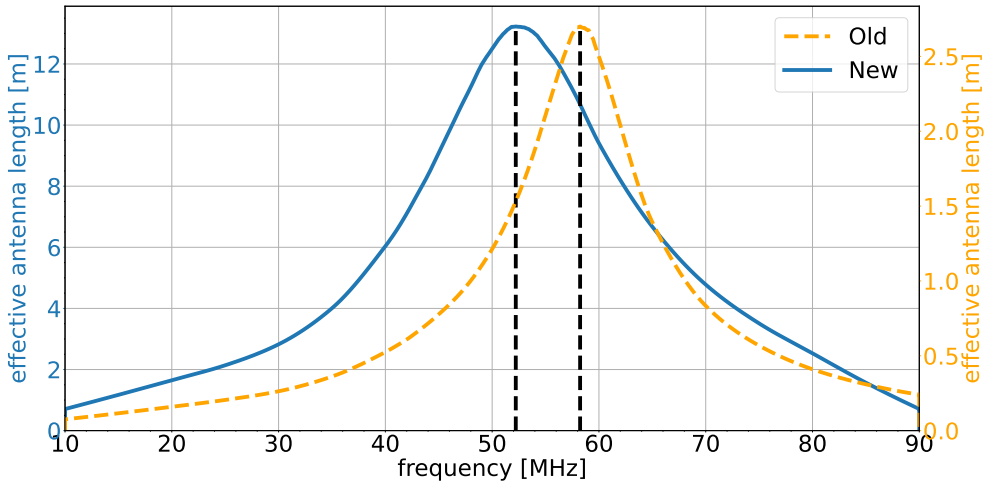

Fig. 4.6: Comparison of the old and the new antenna response by plotting the effective antenna length in meter calculated with the Jones matrix versus the frequency, with marked peaks. On the left y-axis the new version and on the right y-axis the old one.

Once the code is modified, the antenna response can be illustrated by plotting the Jones matrix versus the frequency as shown in Figure 4.6. It is plotted in comparison with the old version of the antenna response. The shape of the old and new version is quite different. The new one has a much higher effective antenna length than the old one, which is expected due to the added gain of the LNA and it is wider than the old one. The peak of the curve is now at 52.2 MHz which is 6.1 MHz more on the lower end of the frequency spectrums the old one at 58.3 MHz. The resonance peak should be close to the shifted frequency due to the LNA, at 58 MHz [5]. This indicates that the changes made deteriorate the antenna model.

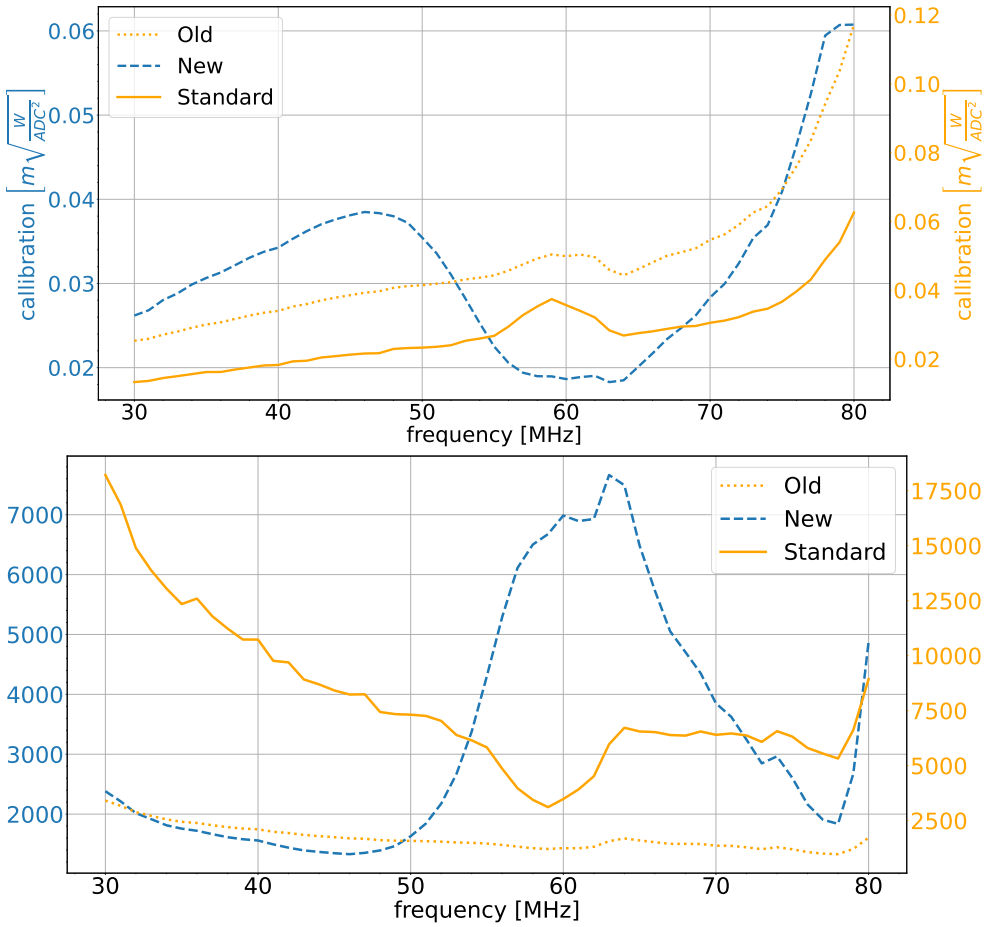

Fig. 4.7: Comparison of calibration of the old, the standard and the new antenna response plotted versus frequency. The one in the top is the calibration curve in $\sqrt{\frac{W}{ADC^2}}$ and the one beneath is the antenna model correction factor (A_X) which is unitless. Both plotted with the new antenna response on the left y-axis and the old and standard one, is the PyCRtools antenna model, on the right y-axis.

To see how the new version is performing a closer look at the frequency dependent calibration, see section 4.2, and how it changes with the new antenna response is necessary. So with a changed in the antenna response a change in the calibration curve is expected. Therefore the new antenna response is plotted in Figure 4.7 in comparison with the unchanged response, used by AARTFAAC and the standard model, which is the PyCRtools antenna model. There it is clearly visible that something is off. The calibration curve is half of the old version of the antenna model. Also it appears a peak between 40 MHz and 50 MHz, where the old ones are a nearly straight line. The steep fall after the peak and the valley at 60 MHz, where the old one had a peak indicates that the code tries to compensate for the new antenna model in that area which should not be necessary.

It becomes clearer if we look at the lower graph in Figure 4.7 which is the antenna model correction factor. There is a big peak in the area of the valley, where none is in the standard and the old antenna model.

So, in conclusion to this, the attempt of putting in the measured impedance Z_{11} for Equation 4.3 and the measured gain S_{21} produced an antenna response that models the antenna not close at all. The influence of the balun on the antenna is way too big to get usable results. But as the balun has most of its influence on the impedance, it is possible that the gain remains in a way usable.

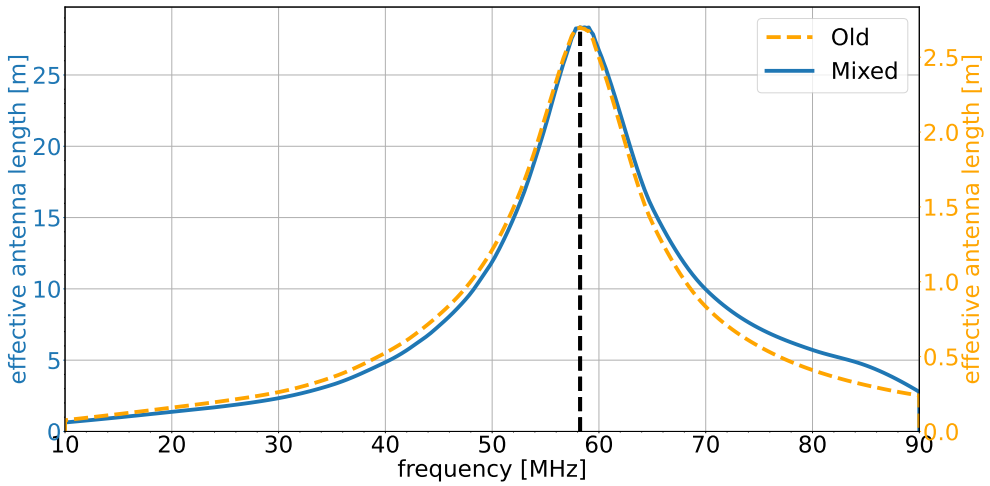

Fig. 4.8: Comparison of the old and the new antenna response by plotting the effective antenna length in meter calculated with the Jones matrix versus the frequency, with marked Peaks. On the left y-axis the mixed version and on the right y-axis the old version.

So, as the antenna response with the measured impedance is not usable, a mixed model will maybe give a better result. In the old antenna response the gain of the antenna is not included, so it could improve the model to change it so that it uses the gain of the LNA, discussed in section 4.3, and the old Z_{LNA} again to calculate the impedance. This change will be referred to as mixed model.
At first taking a closer look at the plotted Jones Matrix, shown in Figure 4.8. There it is visible that the old and mixed antenna response are very similar in shape like expected after the gain adds only a factor to the antenna model. So because of this factor the effective antenna length of the mixed model is way higher than the old model by a factor of 10. Also the peak frequency do not shift is remains at 58.2 MHz where the old peak is. This is as accepted because it still remains at the resonance frequency of the whole LBA at 58 MHz and adding the gain should only effect the amplitude.
To see how good the mixed model is, again a closer look at the calibration curve and the antenna model correction factor is necessary, both are shown in Figure 4.9. The mixed version is now like the shape of the old antenna model. In the calibration curve the old model is slightly higher than the mixed one, but has a steeper climb after 75 MHz. It is positive that all three show the peak at around 58 MHz. At the antenna model correction factor the shape is nearly the same again, only after 78 MHz the old antenna response climbs a lot steeper than the mixed one, which is good. All three have the same peak on the right and same valley at 58 MHz and a peak afterwards, so they have the same characteristics. The peaks at around 60 MHz are expected to be there, because of a resonance that is not calculated for.[6] Both graphs lead to the conclusion that the mixed curve is good, which can be noticed well after looking at how flat the curve is. For the antenna model correction factor a flatter curve is better. As the mixed model does not show the steep climb at the end like the old one does it could be called better.

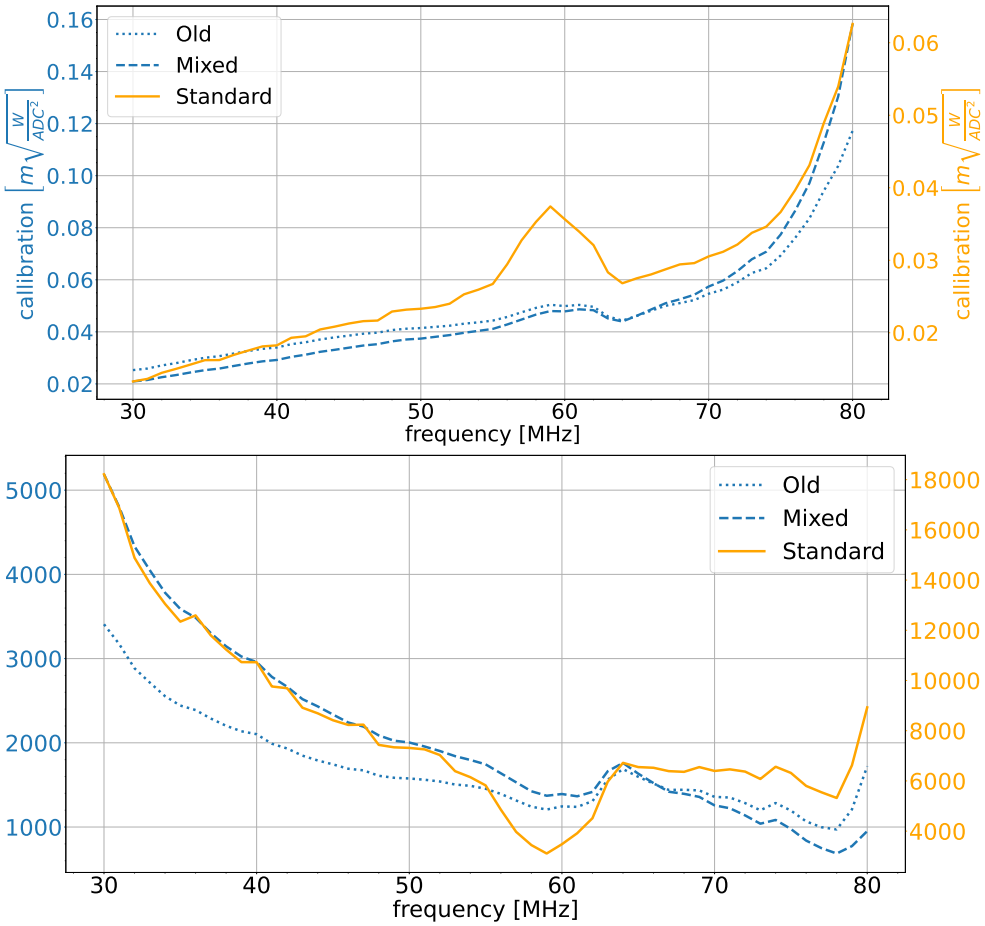

Fig. 4.9: Comparison of calibration of the old, standard and the mixed antenna response plotted versus frequency. The one in the top is the calibration curve in $\sqrt{\frac{W}{ADC^2}}$ and the one beneath is the antenna model correction factor (A_X) which is unit less. Both plotted with the standard antenna response, the PyCRtools antenna model, on the right y-axis and the old and mixed one on the left y-axis.

5 Summary

The aim of this thesis was for a better understanding of the antenna response and for a change of the existing code of the antenna response to work with a more accurate model of the low band antennas used at the LOFAR.

I took a look at the low noise amplifier of the low band antennas from LOFAR. Therefore the LNA was measured with a vector network analyser to see how the scattering parameter and the impedances of the LNA behave over the frequency range of the LBAs in order to make sure the measurements were not too much influenced by the components used in the measurement.

The analysis of the other components in the measurements showed that the used bias tee has a good isolation between the DC-path and the signal path. It was mostly quite flat in its S-parameters, but the impedances depends on the frequency. So over all the bias probably did not influence the measurement to much, but could still be improved. But it turned out that the balun can not be used in the way done. It dominates the impedance way to much and a balun can not be used to measure the LNA per VNA, like tried.

The measurements of the LNA itself showed that the LNA is mostly influenced by cold weather and low and high power outputs. The results show that mostly the gain and the impedances of the LNA are influenced by the frequency. The delay of higher frequency signals is higher than the ones of the group delay, too.

After that the measurements were built in the antenna response model of the AARTFAAC. That changed the plotted Jones Matrices visibly, as well as the calibration curves of the antenna. So with these results it is clear that the balun influenced the measurements of the impedance too much to get any good results to be used in the antenna model. But the measured gain of the LNA is not so much influenced by the balun that it is completely unusable. Therefore a mixed model of the old one and the new one, by just using the gain of the LNA, produced a better result before. So that it is still not perfect or probably good enough for use in application, but it shows that by taking the gain in account a flatter calibration curve can be produced. Therefore it would be a big step forward in the future for the model and calibration if a better measurement of the gain could be accomplished.

In conclusion, in the future, the measurements need to be performed in a better way to understand the amplifier better and model the antenna response better. For correct measurements it is necessary to find another way to measure the LNA. With the improved measurements it could also be good to try to test

the antenna model with cosmic ray data, or maybe as well with the existing one, to verify the model. Since cosmic ray data are measured with LOFAR and also are a part of the research work from LOFAR and therefore are well known. In future the lightning research will make more advances with LOFAR and bring this only little explored field to better results towards understanding one of the most terrifying and beautiful phenomena on earth. Through this work we hope to contribute to absolutely calibrated lightning measurements.

Bibliography

[1] *10 Years of LOFAR highlights*. https://www.astron.nl/wp-content/uploads/2020/12/10yearslofar.pdf. (Accessed on 09/10/2022). June 2020.

[2] *Antennas - ASTRON Science*. https://science.astron.nl/telescopes/lofar/lofar-system-overview/technical-specification/antennas/. (Accessed on 09/04/2022).

[3] *balun, n. : Oxford English Dictionary*. https://www.oed.com/view/Entry/250657. (Accessed on 09/02/2022).

[4] *Bias Tees*. https://info.apitech.com/bias-tees-va. (Accessed on 09/01/2022).

[5] M. P. van Haarlem et al. "LOFAR: The LOw-Frequency ARray". In: *A&A* 556 (2013), A2. DOI: 10.1051/0004-6361/201220873. URL: https://doi.org/10.1051/0004-6361/201220873.

[6] B. M. Hare. Internal Report.

[7] B. M. Hare et al. "Needle-like structures discovered on positively charged lightning branches". In: *Nature* 568.7752 (Apr. 2019), pp. 360–363. ISSN: 0927-6505. DOI: https://doi.org/10.1038/s41586-019-1086-6.

[8] B.M. Hare et al. "Radio Emission Reveals Inner Meter-Scale Structure of Negative Lightning Leader Steps". In: *Physical Review Letters* 124.10 (Mar. 2020). DOI: 10.1103/physrevlett.124.105101.

[9] K. Hübner. *Code Bachelor Thesis*. https://github.com/HueKl/Bachelor-Thesis. access request able over: kl.hue@pm.me.

[10] *Lightning Across the Solar System | Science Mission Directorate*. https://science.nasa.gov/science-news/news-articles/lightning-across-the-solar-system. (Accessed on 09/09/2022).

[11] *LOFAR - ASTRON*. https://www.astron.nl/telescopes/lofar. (Accessed on 09/03/2022).

[12] *LOFAR stations - ASTRON Science*. https://science.astron.nl/telescopes/lofar/lofar-system-overview/technical-specification/lofar-stations/. (Accessed on 09/06/2022).

[13] Vladislav Mazur. *Principles of Lightning Physics*. 2053-2563. IOP Publishing, 2016. ISBN: 978-0-7503-1152-6. DOI: 10.1088/978-0-7503-1152-6. URL: https://dx.doi.org/10.1088/978-0-7503-1152-6.

[14] K. Mulrey et al. "Calibration of the LOFAR low-band antennas using the Galaxy and a model of the signal chain". In: *Astroparticle Physics* 111 (2019), pp. 1–11. ISSN: 0927-6505. DOI: https://doi.org/10.1016/j.astropartphys.2019.03.004. URL: https://www.sciencedirect.com/science/article/pii/S0927650518302810.

[15] A. Nelles et al. "Calibrating the absolute amplitude scale for air showers measured at LOFAR". In: *Journal of Instrumentation* 10.11 (Nov. 2015), P11005–P11005. DOI: 10.1088/1748-0221/10/11/p11005.

[16] O. Scholten et al. "Interferometric imaging of intensely radiating negative leaders". In: *Phys. Rev. D* 105 (6 Mar. 2022), p. 062007. DOI: 10.1103/PhysRevD.105.062007.

[17] O. Scholten et al. "The Initial Stage of Cloud Lightning Imaged in High-Resolution". In: *Journal of Geophysical Research: Atmospheres* 126.4 (Feb. 2021). DOI: 10.1029/2020jd033126.

[18] *scipy.interpolate.interp1d — SciPy v1.9.1 Manual*. https://docs.scipy.org/doc/scipy/reference/generated/scipy.interpolate.interp1d.html. (Accessed on 09/08/2022).

[19] *Vektorielle Netzwerk-Analysatoren werden erschwinglich*. https://www.meilhaus.de/news-aktionen/blog/blog-vna/. (Accessed on 09/01/2022).

Acknowledgments

I would like to thank everyone who helped me to write this thesis.

- Prof. Dr. Anna Nelles, who supported me all the time, always had time for me and provided me with this exciting topic.
- Dr. Brian Hare, who introduced me to the topic and helped me with questions.
- Dr. Adrian Zink, who provided invaluable help in measuring the LNA and provided me with the data I needed for this thesis.
- Dr. Katharine Mulrey, who answered my questions and introduced me to her code.
- Dr. Maddalena Cataldo, who proofread the paper and was always available to answer questions.

My thanks also go to my friends and family who supported me during my work.

Selbstständigkeitserklärung

Hiermit erkläre ich, dass ich die vorliegende Arbeit selbstständig und ohne fremde Hilfe verfasst und keine anderen Hilfsmittel als die angegebenen verwendet habe.

Insbesondere versichere ich, dass ich alle wörtlichen und sinngemäßen Übernahmen aus anderen Werken als solche kenntlich gemacht habe.

Ort, Datum	Klaus Hübner